

# Achieving Polymorphic and Stoichiometric Diversity in Cocrystal Formation: Importance of Solid-State Grinding, Powder X-ray Structure Determination, and Seeding

Andrew V. Trask,<sup>†</sup> Jacco van de Streek,<sup>‡</sup> W. D. Samuel Motherwell,<sup>‡</sup> and William Jones<sup>\*,†</sup>

*Pfizer Institute for Pharmaceutical Materials Science, Department of Chemistry, University of Cambridge, Lensfield Road, Cambridge CB2 1EW, U.K., and Cambridge Crystallographic Data Centre, 12 Union Road, Cambridge CB2 1EZ, U.K.*

*Received April 20, 2005; Revised Manuscript Received August 17, 2005*

**ABSTRACT:** Solid-state grinding is explored as a means of selectively preparing specific stoichiometric or polymorphic modifications of crystalline supramolecular complexes, or cocrystals. In research involving cocrystals of the model pharmaceutical compound caffeine prepared via solid-state grinding and solution crystallization, it has been demonstrated that these two methods of preparation are not always coterminous with respect to the cocrystal product obtained. Examined herein are the structures of five previously unreported caffeine cocrystals with monocarboxylic acids, including formic acid, acetic acid, and trifluoroacetic acid. This system illustrates three different possibilities in performing cocrystal preparation via the dual methods of solid-state grinding and solution crystallization: (1) the same cocrystal can result from both methods; (2) different cocrystal stoichiometries can result from each method; (3) different cocrystal polymorphs can result from each method. Materials that at first could be prepared only by solid-state grinding were later induced to crystallize from solution by seeding with the grinding material. Because some cocrystals from grinding contained minor residual unreacted starting components, a phase-subtraction method was used to enable subsequent crystal structure determination from powder X-ray diffraction data. The findings herein assign a significance to solid-state grinding as a technique of choice in widespread screening efforts for novel supramolecular materials.

## Introduction

Pharmaceutical cocrystals are crystalline molecular complexes that contain therapeutically active molecules. This class of engineered supramolecular materials has garnered significant interest from the scientific community as an emerging means of tailoring physical properties via supramolecular modification.<sup>1,2</sup> Properties important to the bioavailability and processing of pharmaceutical solids, including solubility and physical stability, have been demonstrated recently to be improved upon via cocrystallization.<sup>3,4</sup> The recent interest in pharmaceutical cocrystals may be attributed to two key advantages that cocrystallization offers over the traditional method of physical property optimization, salt formation. Cocrystal formation is not restricted by requiring an ionizable center on the pharmaceutical molecule, as is the case for salt formation. Additionally, in contrast to the limited number of salt-forming counterions in use today,<sup>5</sup> there exists a relatively large number of biologically nontoxic cocrystallizing molecules available for use in complexation with pharmaceuticals.<sup>6</sup> Combined, the inherent advantages of pharmaceutical cocrystallization indicate a significant impact on the development of tomorrow's medicines.

The great number of potential cocrystallizing molecules simultaneously presents a benefit and a chal-

lenge. The many possible molecular combinations offer increased likelihood of producing new pharmaceutically acceptable crystalline materials. On the other hand, the increased possibilities lead to a complication in the screening for new cocrystal forms. For the traditional method of crystallization from solution, an appropriate solvent must be identified in which each component is suitably soluble while simultaneously promoting cocrystal formation; the large number of possible solvents necessitates a great variety of screening experiments. Automated high-throughput screening has been offered as one means of addressing the increased experimental burden.<sup>7</sup> In the present report, pharmaceutical cocrystal preparation by solid-state grinding is described as a potential means by which the experimental burden of cocrystal screening may be reduced. Moreover, it is observed that solid-state grinding may also provide a means of obtaining novel pharmaceutical cocrystal materials apparently not readily accessible via solution-based screening efforts.

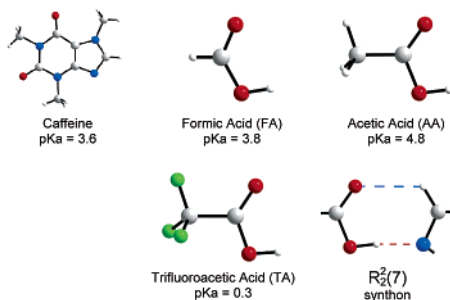
Cocrystal formation by solid-state grinding<sup>8</sup> is certainly not new: a late 19th century report is often cited as the earliest reference to such a procedure.<sup>9</sup> The topic of cocrystal formation by solid-state grinding was addressed in detail by Etter and co-workers. A series of publications demonstrated, *inter alia*, that while many cocrystal materials could be prepared both by solid-state grinding and by solution growth, some could be prepared only by solid-state grinding,<sup>10,11</sup> and conversely, at least one could be prepared only by solution growth.<sup>12</sup> A more recent literature report illustrates that, in certain instances, different products may result from different

\* Corresponding author. Mailing address: Department of Chemistry, University of Cambridge, Lensfield Road, Cambridge CB2 1EW, United Kingdom. Tel: +44 (0) 1223 336 468. Fax: +44 (0) 1223 336 362. E-mail: wj10@cam.ac.uk. Web: <http://www.ch.cam.ac.uk/CUCL/staff/wj.html>.

<sup>†</sup> University of Cambridge.

<sup>‡</sup> Cambridge Crystallographic Data Centre.

### Scheme 1. Cocrystallizing Molecules and Anticipated Heteromeric Synthon



cocrystal preparation methods.<sup>13</sup> It has been reported that cocrystal material at first obtained exclusively by one approach may be used as seeds to subsequently obtain that cocrystal by another method, thereby potentially enabling XRD structure determination via single-crystal growth.<sup>14–16</sup> In one alternative case, cocrystal structure determination was achieved even when material could be prepared only as crystalline powder by grinding.<sup>17</sup>

Of pharmaceutical relevance is an example involving the solid-state grinding preparation of several pharmaceutical cocrystals of the drug sulfadimidine with carboxylic acids.<sup>18</sup> That the cocrystals in that study could also be prepared by solution methods enabled growth of crystals of sufficient size for single-crystal X-ray diffraction (XRD) structure determination. Recent reports have provided evidence for enhanced cocrystallization selectivity in a grinding experiment by the addition of minor quantities of solvent, termed solvent-drop grinding.<sup>4,19</sup> However, to our knowledge, the observation that a pharmaceutical cocrystal material may be obtained exclusively by solid-state grinding has not yet been described.

In the system reported upon here, cocrystals of the model pharmaceutical compound caffeine<sup>20,21</sup> were prepared with formic acid (FA), acetic acid (AA), and trifluoroacetic acid (TA). The cocrystal design was rationally based upon a known, robust acid–base supramolecular synthon, the  $R_2^2(7)$  intermolecular hydrogen bond motif, shown in Scheme 1, together with the cocrystallizing molecules and their corresponding aqueous dissociation constants.<sup>22</sup> The  $R_2^2(7)$  motif has been successfully implemented in crystal engineering strategies with caffeine previously, using dicarboxylic acids.<sup>4</sup> Based upon this hydrogen bonding arrangement, it was initially anticipated that 1:1 stoichiometry would prevail in the resultant cocrystals.

To obtain detailed structural information on several of the materials prepared by solid-state grinding, the method of crystal structure determination from powder X-ray diffraction (PXRD) data was used.<sup>23</sup>

The acids used in this study are liquids at ambient temperature, justifying the term “solvate” as an alternative to “cocrystal” as a descriptor of the crystalline complexes reported here. The distinction is a matter of nomenclature. From the practical standpoint of pharmaceutical materials chemistry, solvate formation has historically been an unplanned, undesirable outcome of a crystallization, whereas cocrystal formation is gaining precedence as a premeditated strategy by which one may surmount physicochemical property challenges of

active pharmaceutical ingredients. The latter description best fits the results presented herein.

### Experimental Section

**Materials.** Caffeine (99% chemical purity) and TA (99%) were sourced from Sigma-Aldrich (Gillingham, U.K.), and FA (98%) and AA (99%) originated from Fisons Scientific (Loughborough, U.K.). All were used as received.

**Caffeine.** PXRD analysis of anhydrous caffeine agreed with that of previously analyzed  $\beta$ -caffeine.<sup>21</sup>

**Cocrystal A (2:1 Caffeine/Formic Acid).** This material was prepared by both solution crystallization and solid-state grinding. Caffeine (220 mg) and FA (1 equiv) were combined in chloroform (ca. 10 mL) and heated to produce a clear, colorless solution. To this solution was added an equal volume of *n*-hexane. Precipitation commenced upon cooling to ambient temperature. Solids were vacuum filtered. Crystals of suitable size for single-crystal XRD were obtained by slow evaporation of a small (ca. 1 mL) aliquot of the chloroform solution that had been removed prior to hexane addition. Solid-state grinding of caffeine (172 mg) and FA (1 equiv) or, alternatively, caffeine (167 mg) and FA (0.5 equiv) for 60 min by the procedure described below produced a powder with a PXRD pattern matching that simulated from the single-crystal structure.

**Cocrystal B (1:2 Caffeine/Acetic Acid).** Single crystals of cocrystal **B** were obtained by dissolving anhydrous caffeine in a large excess of AA with heat and evaporating slowly. Cocrystal **B** could also be prepared by grinding caffeine (145 mg) and AA (2 equiv) for 60 min.

**Cocrystal C (1:1 Caffeine/Acetic Acid)** Attempts at solution crystallization of cocrystal **C** were unsuccessful: equimolar solutions of caffeine and AA in a number of solvents resulted in the precipitation of crystalline caffeine. Solid-state grinding was the only route to this cocrystal, performed by grinding caffeine (146 mg) and AA (1 equiv) for 60 min. Residual “unreacted” caffeine was always present as a minor component in samples of cocrystal **C** that had been prepared by grinding. It was found that the addition of minor quantities of *n*-heptane (38 mg or 4 drops from a pipet) reduced the amount of residual caffeine, as judged by the relative PXRD peak intensities, without otherwise affecting the grinding cocrystallization. Solvent-drop addition has previously been shown to accelerate the kinetics of solid-state grinding cocrystallization.<sup>24</sup>

**Cocrystal D (1:1 Caffeine/Trifluoroacetic Acid, Form I)** Solid-state grinding preparation of cocrystal **D** was performed by grinding caffeine (145 mg) with TA (1 equiv) for 60 min. Following solid-state grinding preparation, it was found that **D** could be prepared as phase-pure material by seeding a saturated solution of caffeine (202 mg) in TA (266 mg) with material prepared by solid-state grinding as above.

**Cocrystal E (1:1 Caffeine/Trifluoroacetic Acid, Form II)** Cocrystal **E** was prepared by grinding together caffeine (298 mg) and TA (1 equiv) for 90 min. The total quantity of material in the grinding jar was determined to be important to the formation of **E**, as discussed in the Results section. In one instance, caffeine dissolved in excess hot TA on a microscope slide crystallized upon cooling as crystals of **E**; however, the repetition of this experiment on a larger scale resulted in a physical mixture of **D** and **E**. Cocrystal **E** could be reliably prepared by seeding a saturated solution of caffeine (201 mg) in TA (273 mg) with seeds of **E** prepared by grinding. It was in this way that a single crystal of **E** was obtained for XRD analysis.

**General Methods.** Solid-state grinding was performed with a Retsch MM200 Mixer Mill, equipped with 10 mL stainless steel grinding jars and two 7 mm stainless steel grinding balls per jar. All grinding was performed at a rate of 30 Hz. The external temperature of the grinding jars at the conclusion of the grinding experiments did not exceed ca. 30 °C.

Routine PXRD data was collected on a Philips X'Pert Pro diffractometer, using Ni-filtered Cu K $\alpha$  radiation ( $\lambda = 1.5418$

Table 1. Summary of Cocrystallization Results

cocrystal designator	A	B	C	D	E
description	2:1 caffeine/FA	1:2 caffeine/AA	1:1 caffeine/AA	1:1 caffeine/TA, form I	1:1 caffeine/TA, form II
method of preparation	solid-state grinding and solution crystallization	solid-state grinding and solution crystallization	solid-state grinding	solid-state grinding and seeded solution crystallization	solid-state grinding and seeded or unseeded solution crystallization
method of crystal structure determination	single-crystal XRD	single-crystal XRD	PXRD	PXRD	single-crystal XRD (and PXRD)
exptl formula	C <sub>8</sub> H <sub>10</sub> N <sub>4</sub> O <sub>2</sub> ·0.5(CH <sub>2</sub> O <sub>2</sub> )	C <sub>8</sub> H <sub>10</sub> N <sub>4</sub> O <sub>2</sub> ·2(C <sub>2</sub> H <sub>4</sub> O <sub>2</sub> )	C <sub>8</sub> H <sub>10</sub> N <sub>4</sub> O <sub>2</sub> ·C <sub>2</sub> H <sub>4</sub> O <sub>2</sub>	C <sub>8</sub> H <sub>10</sub> N <sub>4</sub> O <sub>2</sub> ·C <sub>2</sub> HO <sub>2</sub> F <sub>3</sub>	C <sub>8</sub> H <sub>10</sub> N <sub>4</sub> O <sub>2</sub> ·C <sub>2</sub> HO <sub>2</sub> F <sub>3</sub>
formula weight	217.21	314.30	254.24	308.23	308.23
crystal system	monoclinic	monoclinic	Unit Cell		triclinic
space group	<i>P</i> 2 <sub>1</sub> / <i>c</i>	<i>C</i> 2/ <i>m</i>	orthorhombic <i>Pnma</i>	orthorhombic <i>P</i> 2 <sub>1</sub> 2 <sub>1</sub>	<i>P</i> 1
<i>a</i> (Å)	6.8442(1)	18.1127(8)	9.083 10(20)	23.853 05(75)	9.0006(2)
<i>b</i> (Å)	17.5924(4)	6.4397(3)	6.572 60(8)	12.404 48(31)	9.4853(2)
<i>c</i> (Å)	16.3439(5)	13.4032(8)	20.065 39(51)	4.542 73(8)	16.0190(5)
$\alpha$ (deg)	90	90	90	90	88.637(1)
$\beta$ (deg)	98.248(1)	109.446(2)	90	90	76.862(1)
$\gamma$ (deg)	90	90	90	90	78.423(1)
<i>V</i> (Å <sup>3</sup> )	1947.55(8)	1474.18(13)	1197.9(7)	1344.1(11)	1304.36(6)
<i>Z</i>	8	4	4	4	4
	Single-Crystal XRD Structure Determination		PXRD Structure Determination	PXRD Structure Determination	Single-Crystal XRD Structure Determination
$\theta$ range (deg)	3.61–27.49	3.57–27.48	$\chi^2 = 4.22$	$\chi^2 = 7.57$	3.54–27.55
data/restraints/params	4448/1/289	1808/2/137			5836/24/443
$\rho_{\text{calc}}$ (g cm <sup>-3</sup> )	1.482	1.416			1.564
<i>T</i> (K)	180(2)	180(2)	ambient	ambient	180(2)
<i>R</i> <sub>1</sub>	0.0752	0.0473			0.0916
<i>wR</i> <sub>2</sub>	0.2110	0.1312	degrees of freedom = 6	degrees of freedom = 12	0.2952
physical stability upon ambient storage	stable	stable	dissociation into crystalline caffeine and AA vapor ca. 1 day	stable	polymorph conversion to <b>D</b> ca. 3 days

Å) at 40 kV and 40 mA with an X'Celerator RTMS detector. Each sample was analyzed between 4° and 40° 2 $\theta$  with a step size of 0.017° 2 $\theta$  and a total scan time of 3 min, 5 s. Experimental PXRD patterns were compared to PXRD patterns simulated from available crystal structures to confirm the composition of those materials.<sup>25</sup>

High-resolution PXRD scans for crystal structure determinations were collected on the above instrument, but with monochromatic X-ray Cu K $\alpha$ <sub>1</sub> radiation ( $\lambda = 1.540 56$  Å) generated with an incident focusing beam Johansson monochromator using a Ge(111) crystal. Samples were prepared for collection by filling the crystalline powder into a 0.5 mm diameter borosilicate glass capillary. Each filled, spinning capillary was analyzed at ambient temperature between 5° and 60° 2 $\theta$  with a step size of 0.017° 2 $\theta$  and a total scan time of 16.5 h.

Single-crystal X-ray diffraction data was collected at 180(2) K with a Nonius Kappa CCD diffractometer using Mo K $\alpha$  radiation ( $\lambda = 0.710 73$  Å) and equipped with an Oxford Cryosystems cryostream. Data reduction and cell refinement were performed with the programs *DENZO*<sup>26</sup> and *COLLECT*.<sup>27</sup> Multiscan absorption corrections were applied with the program *SORTAV*.<sup>28</sup> Structures were solved by direct methods using *SHELXS-97*<sup>29</sup> and refined on *F*<sup>2</sup> against all data using *SHELXL-97*.<sup>30</sup> All non-hydrogen atoms were refined with anisotropic displacement parameters. In cocrystals **A** and **B**, the OH hydrogen atoms were located in difference Fourier maps, fixed at an O–H distance of 1.00 Å, and refined isotropically; other hydrogen atoms were placed geometrically and were allowed to ride during subsequent refinement.

Crystal structure determination from PXRD was required for cocrystals **C**, **D**, and **E**, all of which were prepared by solid-state grinding (although a single crystal of **E** was eventually

obtained). In each of these three cases, however, not all the starting material in the grinding jar had cocrystallized. This resulted in the presence of anhydrous caffeine as an impurity phase (as each of the acids in this study are liquids, their possible presence as impurities did not impact the PXRD analysis). The usual way to deal with the presence of an impurity phase is to subtract its fitted profile from the experimental powder pattern, but because the unit cell and crystal structure of anhydrous  $\beta$ -caffeine are not known,<sup>31</sup> this was not possible. Therefore, a high-resolution PXRD pattern of crystalline anhydrous  $\beta$ -caffeine was collected as described above and subtracted from the high-resolution PXRD patterns for cocrystals **C**, **D**, and **E**. All four patterns had been measured for the same 2 $\theta$  values, and the new intensities and estimated standard deviations were calculated as  $I = I_{\text{cocrystal}} - kI_{\text{caffeine}}$  and  $\sigma = \sqrt{(\sigma_{\text{cocrystal}}^2 + (k\sigma_{\text{caffeine}})^2)}$ , respectively, where  $\sigma_{\text{cocrystal}} = \sqrt{I_{\text{cocrystal}}}$  and  $\sigma_{\text{caffeine}} = \sqrt{I_{\text{caffeine}}}$ . The scaling factor *k* was determined by adjusting the overall weight of the caffeine pattern until the known caffeine peaks appeared visually to have been fully removed from the cocrystal pattern.

The impurity-subtracted PXRD patterns thus obtained were subsequently used for structure determination with the program *DASH*.<sup>32</sup> The backgrounds were subtracted with a Bayesian high-pass filter.<sup>33</sup> Peak positions for indexing were obtained by fitting with an asymmetry-corrected Voigt function, followed by indexing with the program *DICVOL*.<sup>34</sup> Pawley refinement was used to extract integrated intensities and their correlations, from which the space groups were determined using Bayesian statistical analysis.<sup>35</sup> Two space groups, *Pnma* and *Pn*2<sub>1</sub>*a*, were returned for cocrystal **C**, and both were tried. The background subtraction, peak fitting, indexing, Pawley refinement, and space-group determination algorithms used are as implemented in the program *DASH*.

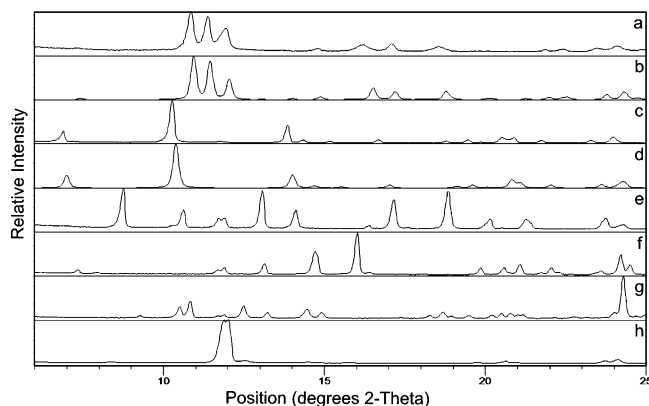


**Figure 1.** PXRD pattern comparison of (a) cocrystal **A** via grinding, (b) cocrystal **A** simulated from single-crystal data, (c) cocrystal **B** via grinding, (d) cocrystal **B** simulated from single-crystal data, (e) cocrystal **C** via grinding, (f) cocrystal **D** via grinding, (g) cocrystal **E** via grinding, and (h) anhydrous caffeine.

Simulated annealing was used to solve the crystal structures from the powder patterns in direct space. Starting molecular geometries were obtained by energy minimization at the VWN-BP/DNP level of theory using the density functional theory program DMol3.<sup>36</sup> Cocrystals **C** and **D** were solved with the standard settings in DASH: 10 runs of 10 000 000 Monte Carlo moves each. The simulated annealing for cocrystal **E**, with four molecules in the asymmetric unit, was set up with 99 runs of 100 000 000 Monte Carlo moves each.

When choosing *Pnma* for cocrystal **C**, we constrained both the caffeine and the AA molecule by symmetry to lie on a mirror plane. Suitable constraints were therefore included in the simulated annealing runs for that space group, namely, fixing the *y*-coordinates for both molecules at  $1/4$ , setting all the occupancies to  $1/2$  (except for some of the hydrogen atoms), and allowing rotations around the *b*-axis only. Imposing these constraints reduces the number of degrees of freedom from 12 to 6.

Final rigid-body Rietveld refinement was carried out by allowing variation in positions and orientations of the molecules, as well as flexible torsion angles, to achieve the best  $\chi^2$  value. Due to the presence of some residual diffraction peaks from the caffeine pattern, it was not justified to allow valence angles and bond lengths to vary, and these were fixed at their calculated starting geometries.

## Results and Discussion

The interesting features pertaining to the synthesis and crystal structure of each of the five caffeine cocrystals are described in turn below, followed by a general discussion on the subject of potential structure–property relationships and the particular opportunities afforded by employing solid-state grinding in the search for novel cocrystals. Details of cocrystals **A–E** are summarized in Table 1. The PXRD patterns for the materials described below are provided in Figure 1.

**Cocrystal A–Caffeine/Formic Acid (2:1).** Cocrystal **A** could be prepared either by solution growth or by solid-state grinding. In the structure, the predicted  $R^2_2$ -(7) caffeine/acid hydrogen bond motif was observed, as can be seen in the row labeled “a” in the crystal packing diagram of cocrystal **A** (Figure 2). The carboxylic acid hydrogen was located in the X-ray difference map on the carboxylic acid, indicating that ionization (proton transfer to the basic nitrogen of caffeine) had not occurred and that **A** is indeed a cocrystal as opposed to a salt. The overall 2:1 caffeine/FA stoichiometry was

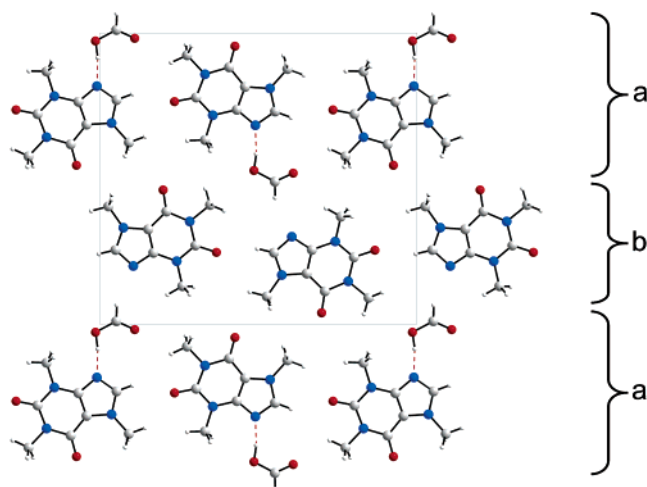


**Figure 2.** Crystal packing diagram of cocrystal **A**, showing alternating rows (a, b) of strongly and weakly hydrogen-bonded interactions. Strong hydrogen bonds are shown as dashed red lines.

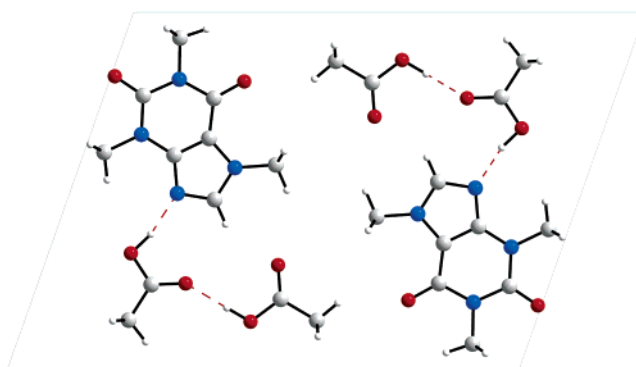


**Figure 3.** Crystal packing of cocrystal **B**, 1:2 caffeine/AA.

unexpected. This stoichiometry results from the inclusion of a second row of caffeine molecules in the structure, in which caffeine is not associated with any conventional “strong” hydrogen bonds. Rather, it appears that a number of weaker hydrogen bonds contribute to the packing of this row of molecules. The weaker interactions include a C–H $\cdots$ O caffeine–caffeine head-to-tail interaction that repeats along row b and a possible C–H $\cdots$ N interaction from the formyl hydrogen to the basic nitrogen of caffeine that repeats perpendicular to b. This cocrystal was observed by PXRD analysis to be physically stable over the course of 6 months of storage under ambient conditions.

It does not appear likely that a 1:1 stoichiometry exists for the caffeine/FA system, because grinding of a 1:1 ingoing ratio of material results in the same cocrystallization product (with excess unreacted acid) as grinding a 2:1 ingoing ratio. Cocrystal **A** represents what appears to be the typical case, in that the same cocrystal product may be obtained either by solution or solid-state grinding methods. The following examples illustrate the more unusual, yet interesting, case in which the different methods produce different cocrystals.

**Cocrystals B and C–Caffeine/Acetic Acid (1:2 and 1:1).** When cocrystallization of caffeine and AA was attempted by growth from a saturated solution of caffeine in excess AA, suitable single crystals of cocrystal

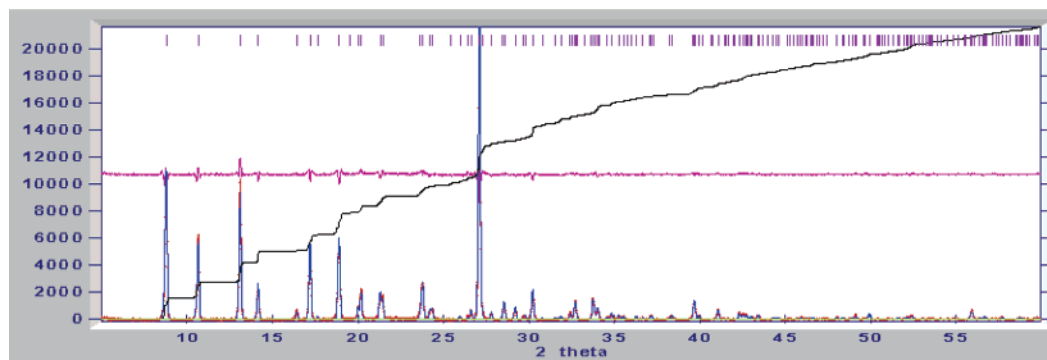


**Figure 4.** Fit of the calculated to the experimental PXRD pattern after rigid-body Rietveld refinement for cocrystal **C**. Calculated (blue), observed (red), and difference (magenta) profiles are shown. Tick marks are shown in purple; the cumulative  $\chi^2$  is shown in black.

**B** resulted, and its crystal structure was solved by single-crystal XRD. Like cocrystal **A**, cocrystal **B** was unexpected in that it did not exhibit 1:1 stoichiometry. The 1:2 caffeine/AA stoichiometry is apparent in the crystal packing of cocrystal **B** (Figure 3). The desired  $R^2_2(7)$  motif is observed in the structure; however, an additional AA molecule participates to form an extended hydrogen bond interaction. Both acidic hydrogens were located in the single-crystal XRD structure solution, confirming that cocrystal **B** is a neutral cocrystal.

Cocrystal **B** could also be prepared by solid-state grinding a 1:2 mixture of caffeine and AA, as judged by a comparison with the simulated PXRD pattern from the single-crystal structure. Over the course of 6 months of storage at ambient conditions, cocrystal **B** exhibited significant physical stability, showing only trace evidence by PXRD of dissociation into crystalline caffeine and AA.

Given the unexpected stoichiometry of cocrystal **B**, it seemed possible that a 1:1 caffeine/AA cocrystal might also exist. However, efforts at growing such a cocrystal from an equimolar mixture of caffeine and AA from a variety of solvents resulted only in crystalline caffeine. Solid-state grinding experiments offered more success. Experiments in which caffeine and AA were ground together in the desired 1:1 ratio resulted in a new PXRD pattern, distinct from that of cocrystal **B**. This material is designated here as cocrystal **C**. A crystal structure of cocrystal **C** was desired to enable a structural comparison to **B**. Clearly, if the cocrystal could not be prepared by solution growth, then single-crystal XRD analysis was not possible. Effort therefore turned to structure determination via PXRD.

The grinding cocrystallization of cocrystal **C** could not be made to go to completion, and excess crystalline anhydrous caffeine could be observed in the PXRD pattern. Efforts to drive the reaction to completion by increased grinding time were ineffective; it appeared as if the cocrystallization had reached an equilibrium point. Attempts to induce the residual caffeine to cocrystallize by introducing excess AA resulted in the emergence of minor quantities of cocrystal **B**, which had been observed to preferentially form when grinding caffeine with two molar equivalents of AA.

As described in the Experimental Section, the phase-impurity subtraction method preceded crystal structure determination from PXRD data. The starting molecules for the simulated annealing procedure were chosen to

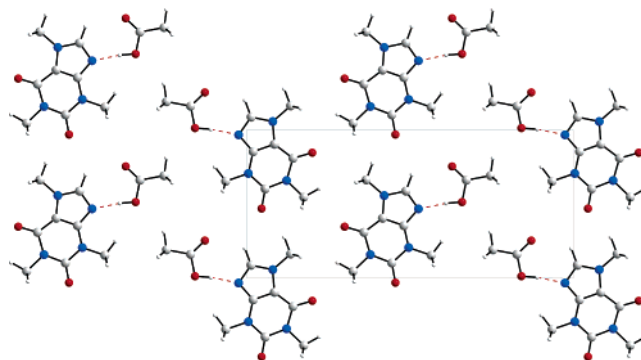


**Figure 5.** Packing diagram of cocrystal **C**, 1:1 caffeine/AA, viewed down [010].

be neutral (unionized) caffeine and AA, with the assumption that the observed neutral character of cocrystal **B** made this situation more likely. (The low scattering power of a hydrogen atom is such that it is typically not possible to determine the ionization state of a complex directly from PXRD structure determination.) Simulated annealing in space groups  $Pnma$  and  $Pn2_1a$  gave almost identical crystal structures. In both space groups, the caffeine molecule lies on a mirror plane. In  $Pnma$ , so does the AA molecule, forced by the space group symmetry; in  $Pn2_1a$ , the AA molecule deviates slightly from the mirror plane but with negligible improvement of the fit to the experimental powder pattern despite having twice as many degrees of freedom available. Combined with the observation that in structure **B** the AA molecule also lies on a mirror plane, the selection of the space group  $Pnma$  appears justified. The correct solution was found six out of 10 times, the remaining four solutions differing only in the orientation of the AA molecule by  $120^\circ$  or  $240^\circ$ . There are no close contacts other than the expected  $R^2_2(7)$  synthon. The excellent fit is shown in Figure 4; the final profile  $\chi^2$  is 4.22.

The crystal structure of cocrystal **C** illustrates the 1:1 stoichiometry (Figure 5). The packing of caffeine and AA in cocrystal **C** reveals the familiar  $R^2_2(7)$  hydrogen bond motif. Channels of AA and caffeine molecules are seen running along the  $a$ -axis. In significant contrast to the physical stability of cocrystal **B**, cocrystal **C** was observed to have largely dissociated into crystalline caffeine and AA vapor after 1 day of storage at ambient conditions in a sealed vial.

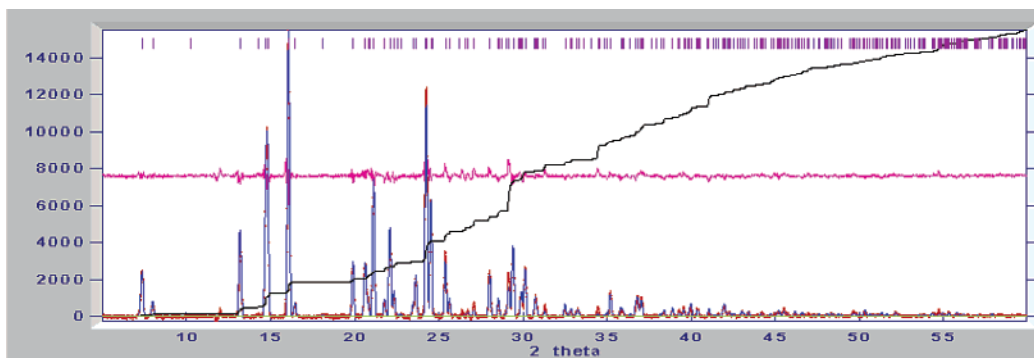


**Figure 6.** Fit of the calculated to the experimental PXRD pattern after rigid-body Rietveld refinement for cocrystal **D**. Calculated (blue), observed (red), and difference (magenta) profiles are shown. Tick marks are shown in purple; the cumulative  $\chi^2$  is shown in black.

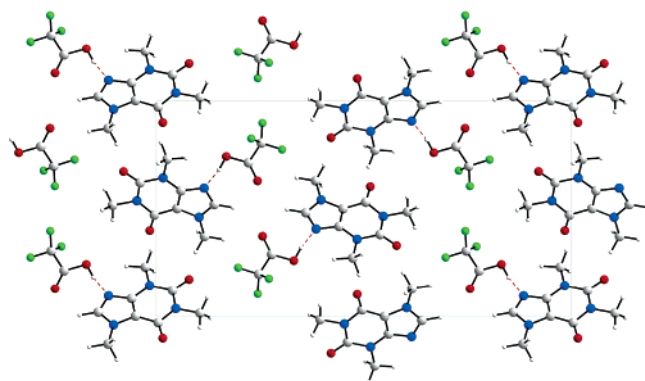


**Figure 7.** Crystal packing of cocrystal **D** (1:1 caffeine/TA, form I) as viewed down [001].

**Cocrystals D and E—Caffeine/Trifluoroacetic Acid (Polymorphs I and II).** Initially, the only successful method of preparing cocrystal **D** (1:1 caffeine/TA) was by solid-state grinding an equimolar mixture of caffeine and TA. The PXRD pattern of this material contained a minor quantity of residual anhydrous caffeine, so prior to PXRD structure solution, it was subjected to the phase-impurity method as described in the Experimental Section. The correct solution was found eight out of 10 times; the other two solutions had a profile  $\chi^2$  that was twice as large. There are no close contacts other than the expected  $R^2_2(7)$  synthon. The fit is shown in Figure 6; the final profile  $\chi^2$  is 7.57. The resulting crystal structure of cocrystal **D** (Figure 7) is similar to the structure of cocrystal **C**, in that both possess alternating zones of acid and caffeine molecules.

In the course of the 1:1 caffeine/TA grinding experiments an interesting observation arose: variation of the total quantity of material in the grinding jar affected the outcome of the cocrystallization experiment. It was observed over the course of about 20 grinding experiments that a smaller quantity of starting material per grinding jar (ca. 140 mg caffeine with 1 equiv of TA) favored formation of cocrystal **D**, while a larger amount (ca. 320 mg caffeine with 1 equiv of TA) resulted in material exhibiting a new PXRD pattern. Total grinding time did not appear to be a factor, as the observation held for total grinding times of 30, 60, and 90 min.

The new PXRD pattern was found to correspond to a polymorph of cocrystal **D**, termed here cocrystal **E**. It was indexed as triclinic,  $Z' = 2$ . During structure solution from PXRD data, the positions and orientations

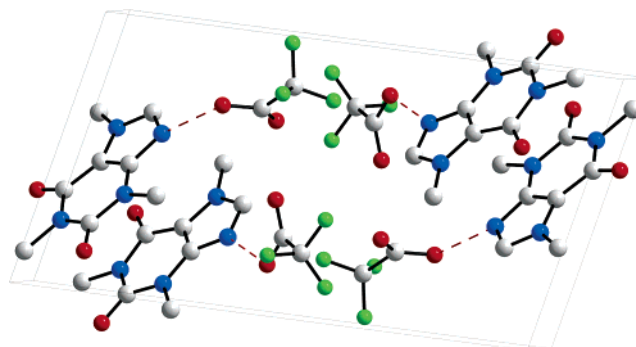


**Figure 8.** Crystal packing of cocrystal **E** (1:1 caffeine/TA, form II), containing two caffeine and two TA molecules per asymmetric unit. Hydrogen atoms and fluorine disorder have been omitted from the diagram for clarity.

of the two caffeine molecules were found to be reproducible as were the positions of the TA molecules, but the orientations of the two TA molecules were not. A single crystal was sought to confirm that part of the crystal structure.

Attempts to cocrystallize from a solution containing 1:1 caffeine/TA in a number of solvents resulted either in crystalline caffeine or occasionally in a material with a different PXRD pattern that could not be reproducibly prepared or fully characterized due to physical instability.<sup>37</sup> Evaporation of a solution of caffeine in excess TA often led to a viscous liquid from which no crystals precipitated. It was found with further experimentation that seeding of this viscous liquid with cocrystals of either **D** or **E** prepared from grinding allowed the preparation of essentially phase-pure samples of either of these cocrystals. In one instance, crystals of cocrystal **E** suitable for single-crystal XRD analysis were obtained in this manner and were used in crystal structure determination (Figure 8). The general features of the single-crystal structure of cocrystal **E** agree with the structure obtained from the PXRD solution. In the single-crystal XRD structure, a considerable amount of disorder in both TA molecules existed; in contrast, the two caffeine molecules are well described (Figure 9).

Given the acidic strength of TA, it was possible that structures **D** and **E** could be ionized salts as opposed to neutral cocrystals. Determining the correct position for the hydrogen atom presented a challenge. The X-ray scattering power of a hydrogen atom is not sufficiently strong as to allow for reliable proton location using

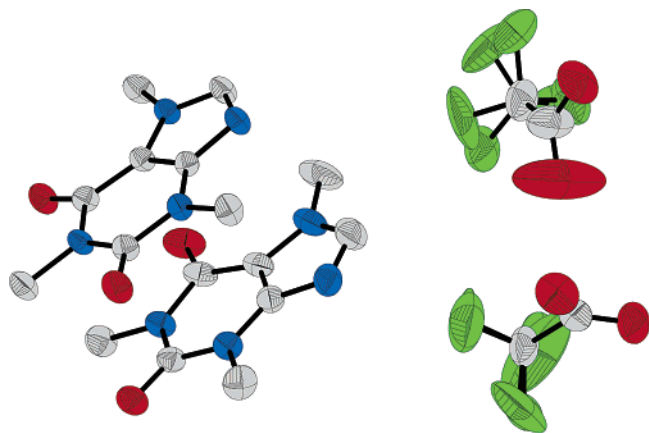


**Figure 9.** ORTEP representation of the four molecules in the asymmetric unit of cocrystal **E** drawn at the 50% probability level, as determined by single-crystal XRD. The occupancies of the fluorine atoms were adjusted during structure solution to model their disorder. Hydrogen atoms have been omitted for clarity.

PXRD structure determination. Additionally, with regard to the single-crystal structure of cocrystal **E**, the acidic hydrogen from each TA molecule was not located in the difference map, and the disorder of the TA molecules discouraged an analysis of the C–O bond lengths to discern carboxyl or carboxylate character.

In an alternative approach, the acidic hydrogen location assignment for cocrystal **E** was assessed by evaluating the geometry of the caffeine molecules in the single-crystal XRD structure. Analysis of the Cambridge Structural Database (CSD)<sup>38</sup> revealed that protonation of the five-membered heterocyclic ring would result in an increase in the internal angle of the C=N–C bond angle involving the basic nitrogen of caffeine. The histograms presented in Figure 10 illustrate this result. Applying this finding to cocrystal **E**, in which the angles of the two caffeine molecules are 104.1(2)° and 104.9(3)°, suggests that both caffeine molecules are neutral and that **E** is indeed a cocrystal rather than a salt.<sup>39</sup>

The aforementioned assessment was also employed in assigning the location of the acidic hydrogen of cocrystal **D**, the polymorphic cocrystal of **E**. The assignment for cocrystal **D** was more tenuous than that for cocrystal **E**, because only PXRD data was available for cocrystal **D**. However, cocrystal **D** was deemed a neutral cocrystal by acknowledgment that polymorphs of salts are often salts, while polymorphs of cocrystals are often cocrystals. It must be mentioned that it is possible for a polymorphic system to exhibit crystal-form-dependent protonation behavior; indeed, the polymorphs of anthranilic acid demonstrate such behavior in a single-component system.<sup>40</sup> A third possibility may also be envisaged, whereby a hybrid protonation state exists, that is, the complex is somewhere between a cocrystal and a salt. In exceptional cases, strongly hydrogen-bonded complexes have been shown to demonstrate such intermediate protonation behavior.<sup>41,42</sup> While the assignments here would have been more straightforward with single crystal data from which the hydrogen location could be directly assessed, the conclusions

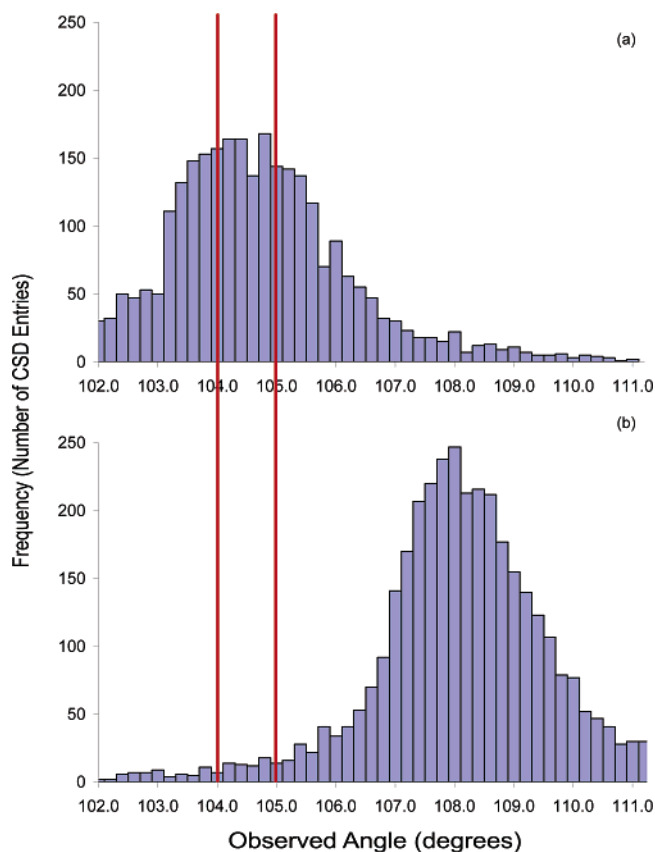


**Figure 10.** Histogram of data from the CSD indicating a trend for the dependence of the internal C=N–C angle of a caffeine-like five-membered heterocyclic on ionization state: (a) neutral ring; (b) protonated ring. The angles of the analogous rings of the two caffeine molecules in cocrystal **E** are indicated by the vertical red lines.

drawn from the available data are provided as a starting point for future investigation into this intriguing system.

It is noteworthy that in cocrystal **E** the anticipated  $R^2_2(7)$  hydrogen bond motif is not observed and that this is the only such instance across the series. While the strong O–H $\cdots$ N hydrogen bond is maintained between both acid–caffeine pairs in the asymmetric unit, the carbonyl moiety of each acid appears to be twisted out of the plane of the corresponding caffeine molecule. In one acid, the carbonyl oxygen bonds to the heterocyclic methylene of a second neighboring caffeine to form a short O $\cdots$ H–C hydrogen bond bridge to a crystallographically inequivalent caffeine. In the other acid, the carbonyl oxygen appears to be directed toward the central carboxylic carbon of the adjacent acid; however, this analysis is complicated by the severe disorder of that particular carbonyl oxygen.

In addition to structural differences, the physical stability of the polymorphic cocrystals **D** and **E** also provided an interesting juxtaposition. While cocrystal **D** was physically stable upon storage at ambient conditions for a period of 6 months, it was found that under the same conditions cocrystal **E** fully converted to cocrystal **D** in as little as 3 days.

**Comparative Analysis and Discussion.** Pharmaceutical cocrystals are attracting attention as a means of tailoring physicochemical properties of drug substances. It is thus of interest here, with structural data

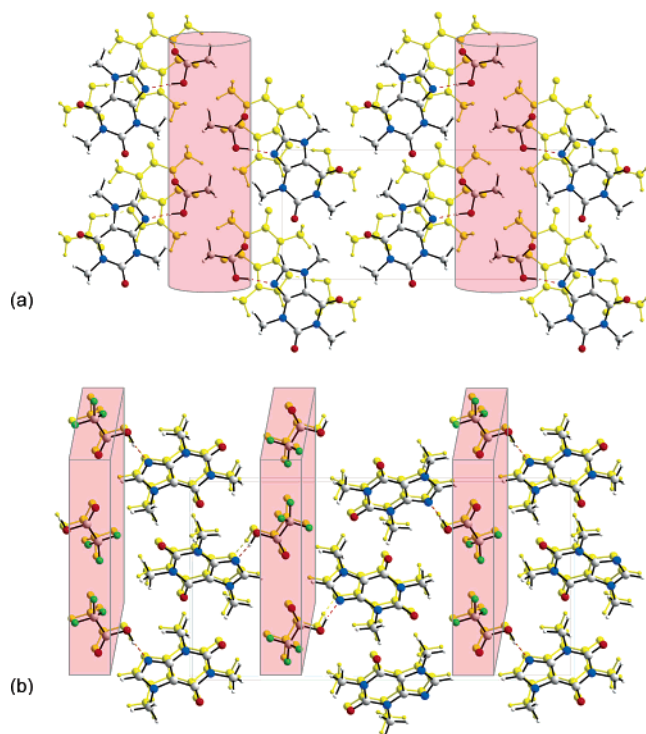


**Figure 11.** Crystal packing diagrams, each showing two overlaid sheets of hydrogen-bonded caffeine/acid units. The underlying sheets have been colored yellow. In cocrystal **C** (panel a), the units are translated between sheets via a screw axis, so vertical channels of AA molecules, in red, may be observed. In cocrystal **D** (panel b), the caffeine/TA sheets directly overlay, leading to orthogonal sheets of TA molecules, depicted in red.

and physical stability observations in hand for a number of related cocrystal materials, to consider potential correlations between the two.

Cocrystals **B** and **C** may be evaluated on the basis that they both possess caffeine/AA interactions, albeit with different stoichiometries. A physical stability difference is clear: while cocrystal **B** was stable upon storage in a sealed vial at ambient temperature for over 6 months, cocrystal **C** was observed at the same storage condition to largely dissociate into crystalline caffeine and AA vapor after 1 day. The variation is remarkable and highlights the wide range of physical stabilities that may result from cocrystal formation with a given active pharmaceutical ingredient. In the search for a physical factor that may underlie the observation, it is noted that the potentially volatile AA molecules lack a direct exit pathway from within the crystal structure of cocrystal **B**. Alternatively, linear channels of AA along [100] may be observed in the structure of cocrystal **C** (Figure 11a), through which it may be envisaged that the AA molecules may diffuse out of the structure, causing its collapse. Thus it is possible that basic packing differences may have contributed to the variation in physical stability between cocrystals **B** and **C**.

A similar analysis may be applied to the pair of 1:1 caffeine/acid cocrystals **C** and **D**, wherein the 1-day physical dissociation of cocrystal **C** contrasts with the 6-month physical stability of cocrystal **D**. The similar hydrogen bonding and crystal packing of cocrystals **C** and **D**, as seen in Figures 5 and 7, illustrate that both cocrystals consist of alternating zones of caffeine and

acid. A closer look at cocrystal **D** reveals that as a result of its crystal packing, TA molecules exist in two-dimensional sheets perpendicular to [100] (Figure 11b). Thus it appears that in both cocrystals **C** and **D**, the acid molecules have a potential route of diffusion from the crystal (via channels and sheets, respectively). As a result, basic packing differences may not underlie the observed stability difference between cocrystals **C** and **D**.

Alternatively, an underlying source of the stability difference between cocrystals **C** and **D** may pertain to the differing strengths of intramolecular interactions in the two cocrystals. Such interactions must include the strength of the caffeine/AA and caffeine/TA hydrogen bond within the  $R^2_2(7)$  motif, which is expected to be a function of the differing proton affinities of the acids.<sup>43</sup> The analysis above suggests that in designing cocrystals for improved physical stability, one must consider as important factors the overall cocrystal packing features as well as the intramolecular interaction differences, including hydrogen bond strength.

In assessment of the opportunities afforded by solid-state grinding in the preparation of new supramolecular materials, a number of observations in this study are of particular interest. The effect of the quantity of material in the grinding jar on the polymorphic outcome of the caffeine/TA system (cocrystals **D** and **E**) is noteworthy and to our knowledge has not previously been reported. No explanation for this observation is offered here, and further study is clearly needed to understand the basis of this effect. In general, a great deal remains to be understood regarding the preparation of cocrystals by solid-state grinding, as has also been indicated by several other recent reports.<sup>13,44,45</sup>

Furthermore, it is noted that the substantially energetic grinding process can be used to produce physically unstable cocrystals. Indeed, cocrystal **E**, which had been prepared by grinding, showed conversion to polymorph **D** upon standing at ambient conditions, and in one instance, polymorph conversion appeared to be induced by gentle manual grinding with a mortar and pestle. Additionally, cocrystal **C**, which was also prepared by solid-state grinding, was sufficiently unstable as to dissociate after 1 day. In contrast, the cocrystals **A**, **B**, and **D**, all of which were stable for at least 6 months of storage, could also be prepared by solid-state grinding. The variety of physical properties obtainable in products prepared by solid-state grinding suggests widespread application in fields pertaining to materials chemistry.

The question of why certain materials in this study could be prepared only by solid-state grinding (or from solution only with grinding seeds) is unanswered here yet remains an important area of future investigation if this phenomenon is to be exploited in other systems. While it was not evidenced in the present work, it should be noted that a report exists of a polymorph transformation of  $\beta$ -caffeine to the metastable  $\alpha$ -caffeine upon grinding,<sup>46</sup> and in general, it is possible that such grinding-induced phase changes could contribute to the formation of one cocrystal form over another. It is also possible that cocrystallization from solution was inhibited by solvent interference in the heteromeric hydrogen-bonding motif necessary for nucleation of the cocrystal material. The introduction of seeds prepared by the

grinding method to the solution cocrystallization may have served to overcome this solvent-based interference. From a practical perspective, since solution crystallization has the potential added advantages of particle size and crystal habit control, as well as possible chemical purification, the ability to prepare new cocrystals via solution growth is an important complement to the use of solid-state grinding as a screening method for novel cocrystal materials.

### Conclusions

Solid-state grinding as applied to the synthesis of novel supramolecular complexes offers a wealth of possibilities for the discovery of novel materials with functional properties. Demonstrated herein is the preparation of five cocrystals of a model pharmaceutical compound that include variations in stoichiometric and polymorphic modification; a wide range of physical stabilities was also observed across the series. Structure determination via PXRD data afforded a molecular-level analysis of these materials and offered potential structure–property insight. Seeding of solutions with materials that at first had been prepared exclusively by solid-state grinding offered an ability to later prepare these materials by the more routine method of solution crystallization, potentially offering wider industrial application.

**Acknowledgment.** John E. Davies is acknowledged for single-crystal XRD data collection and for structure determination assistance. Graeme Day is acknowledged for providing the energy-minimized molecular structures for PXRD structure determination efforts. The authors thank Neil Feeder, Pete Marshall, Amy Gillon, and Martyn Ticehurst for helpful discussions. A.V.T., W.D.S.M., and W.J. thank the Pfizer Institute for Pharmaceutical Materials Science for funding.

**Supporting Information Available:** X-ray crystallographic information files (CIF) are available for cocrystals A–E. This material is available free of charge via the Internet at <http://pubs.acs.org>.

### References

- Almarsson, Ö.; Zaworotko, M. J. *Chem. Commun.* **2004**, 1889–1896.
- Childs, S. L.; Chyall, L. J.; Dunlap, J. T.; Smolenskaya, V. N.; Stahly, B. C.; Stahly, G. P. *J. Am. Chem. Soc.* **2004**, *126*, 13335–13342.
- Remenar, J. F.; Morissette, S. L.; Peterson, M. L.; Moulton, B.; MacPhee, J. M.; Guzmán, H. R.; Almarsson, Ö. *J. Am. Chem. Soc.* **2003**, *125*, 8456–8457.
- Trask, A. V.; Motherwell, W. D. S.; Jones, W. *Cryst. Growth Des.* **2005**, *5*, 1013–1021.
- Stahl, P. H.; Wermuth, C. G. *Handbook of Pharmaceutical Salts: Properties, Selection and Use*; Verlag Helvetica Chimica Acta: Zürich, 2002.
- Such molecules may include food ingredients and additives, vitamins, nutrients, pharmaceutical excipients, biomolecules, and other drug molecules.
- Morissette, S. L.; Almarsson, Ö.; Peterson, M. L.; Remenar, J. F.; Read, M. J.; Lemmo, A. V.; Ellis, S.; Cima, M. J.; Gardner, C. R. *Adv. Drug Delivery Rev.* **2004**, *56*, 275–300.
- Trask, A. V.; Jones, W. In *Topics in Current Chemistry*; Toda, F., Ed.; Springer: Berlin, 2005; Vol. 254, pp 41–70.
- Ling, A. R.; Baker, J. L. *J. Chem. Soc.* **1893**, *63*, 1314–1327.
- Etter, M. C.; Adson, D. A. *Chem. Commun.* **1990**, *8*, 589–591.
- Etter, M. C.; Reutzel, S. M. *J. Am. Chem. Soc.* **1991**, *113*, 2586–2598.
- Etter, M. C.; Reutzel, S. M.; Choo, C. G. *J. Am. Chem. Soc.* **1993**, *115*, 4411–4412.
- Kuroda, R.; Imai, Y.; Tajima, N. *Chem. Commun.* **2002**, 2848–2849.
- Hollingsworth, M. D.; Santarsiero, B. D.; Oumar-Mahamat, H.; Nichols, C. J. *Chem. Mater.* **1991**, *3*, 23–25.
- Hollingsworth, M. D.; Brown, M. E.; Santarsiero, B. D.; Huffman, J. C.; Goss, C. R. *Chem. Mater.* **1994**, *6*, 1227–1244.
- Braga, D.; Maini, L.; Polito, M.; Mirolo, L.; Grepioni, F. *Chem. Commun.* **2002**, 2960–2961.
- Cheung, E. Y.; Kitchin, S. J.; Harris, K. D. M.; Imai, Y.; Tajima, N.; Kuroda, R. *J. Am. Chem. Soc.* **2003**, *125*, 14658–14659.
- Caira, M. R.; Nassimbeni, L. R.; Wildervanck, A. F. *J. Chem. Soc., Perkin Trans. 2* **1995**, 2213–2216.
- Trask, A. V.; Motherwell, W. D. S.; Jones, W. *Chem. Commun.* **2004**, 890–891.
- Griesser, U. J.; Burger, A. *Int. J. Pharm.* **1995**, *120*, 83–93.
- Edwards, H. G. M.; Lawson, E.; de Matas, M.; Shields, L.; York, P. J. *J. Chem. Soc., Perkin Trans. 2* **1997**, 1985–1990.
- The Merck Index*, 13th ed.; Merck & Co.: Whitehouse Station, NJ, 2001.
- David, W. I. F.; Shankland, K.; McCusker, L. B.; Baerlocher, C., Eds. *Structure Determination from Powder Diffraction Data*; Oxford University Press: Oxford, U.K., 2002; Vol. 13.
- Shan, N.; Toda, F.; Jones, W. *Chem. Commun.* **2002**, 2372–2373.
- PXRD patterns simulated using the software X'Pert Plus, version 1.0, Philips Analytical B.V., 1999.
- Otwinowski, Z.; Minor, W. In *Macromolecular Crystallography, Part A*; Carter Jr., C. W., Sweet, R. M., Eds.; Academic Press: San Diego, CA, 1997; Vol. 276, pp 307–326.
- Nonius; Nonius BV: Delft, The Netherlands, 1998.
- Blessing, R. H. *Acta Crystallogr.* **1995**, *A51*, 33–38.
- Sheldrick, G. *SHELXS-97*; University of Göttingen: Germany, 1997.
- Sheldrick, G. *SHELXL-97*; University of Göttingen: Germany, 1997.
- Carlucci, L.; Gavezzotti, A. *Chem.—Eur. J.* **2004**, *11*, 271–279.
- David, W. I. F.; Shankland, K.; Shankland, N. *Chem. Commun.* **1998**, 931–932.
- David, W. I. F.; Sivia, D. S. *J. Appl. Crystallogr.* **2001**, *34*, 318–324.
- Boulton, A.; Louer, D. *J. Appl. Crystallogr.* **1991**, *24*, 987–993.
- Markvardsen, A. J.; David, W. I. F.; Johnson, J. C.; Shankland, K. *Acta Crystallogr.* **2001**, *A57*, 47–54.
- DMol3*; Accelrys Inc.: San Diego, CA, 2004.
- The first 10 peaks of this PXRD pattern, in degrees  $2\theta$ , are 7.92, 10.48, 12.07, 13.06, 15.93, 16.89, 18.75, 20.88, 21.13, and 21.98.
- Allen, F. H. *Acta Crystallogr.* **2002**, *B58*, 380–388.
- Had it been available, better crystallographic data would have allowed hydrogen assignment with greater certainty; nonetheless, IR spectroscopy appears to confirm this assignment for both polymorphs D and E, in that no evidence of carboxylate ion antisymmetric stretching is apparent in the region of ca. 1550–1610  $\text{cm}^{-1}$ . Solid-state NMR ( $^{13}\text{C}$  and  $^{15}\text{N}$ ) analysis is currently underway to further characterize these materials.
- Ojala, W. H.; Etter, M. C. *J. Am. Chem. Soc.* **1992**, *114*, 10288–10293.
- Steiner, T.; Majerz, I.; Wilson, C. C. *Angew. Chem., Int. Ed.* **2001**, *40*, 2651–2654.
- Foces-Foces, C.; Echevarría, A.; Jagerovic, N.; Alkorta, I.; Elguero, J.; Langer, U.; Klein, O.; Minguet-Bonvehí, M.; Limbach, H. H. *J. Am. Chem. Soc.* **2001**, *123*, 7898–7906.
- Gilli, G.; Gilli, P. *J. Mol. Struct.* **2000**, *552*, 1–15.
- Braga, D.; Maini, L. *Chem. Commun.* **2004**, 976–977.
- Kuroda, R.; Higashiguchi, K.; Hasebe, S.; Imai, Y. *CrystEngComm* **2004**, *6*, 463–468.
- Pirttimäki, J.; Laine, E.; Ketolainen, J.; Paronen, P. *Int. J. Pharm.* **1993**, *95*, 93–99.